Report on A.1.1 and B.1.5 experiments: a combined analysis

D. López-Aires[1], J. P. Fernández-García [1,2], M. A. G. Alvarez[1]
[1] *Departamento FAMN, Universidad de Sevilla, Apartado 1065, 41080 Sevilla, Spain and*
[2] *Centro Nacional de Aceleradores, Universidad de Sevilla, Junta de Andalucía-CSIC, 41092 Sevilla, Spain*
(Dated: June 10, 2021)

We report on a common analysis for the experiments of SiPM characterization (A.1.1) and comparison of different scintillating crystals: light yield, decay time and resolution (B.1.5). With this proposal, we use CAEN educational kit premium, based on SP5600 power supply and amplification unit connected to the SP5650C SiPM and the DT5720A digitizer. On one hand, we use the SP5601 LED driver. On another hand we use a ^{137}Cs gamma source coupled individually to BGO, LYSO(Ce) and CsI(Tl) crystals with a constant volume (6x6x15 mm^3). In the former case, we vary the amplitude (intensity) of the LED driver and verify the spectroscopic response. In the latter case, the light yield is due to a ^{137}Cs gamma source interaction with the respective crystal, and again a spectroscopic response is analyzed. As a proof of concept, pulse high and pulse shape analyses are also proposed. Schematic comparisons of the results obtained with the three crystals are presented.

I. INTRODUCTION

For decades, photomultiplier (PM) tubes have been the most common light amplifiers used with scintillators. Semiconductors developments led to the new technology of photodiodes (PD). Photodiodes offer several advantages: high quantum efficiency, lower power consumption, compact size, hardness and insensitivity to magnetic fields. They are configured following 3 main designs: PIN diodes, avalanche photodiodes (APD) and Silicon photomultiplier (SiPM) [1,2]. PIN diodes have no internal gain and operate directly converting photons to electron-hole pairs, being electrons simply collected. Unlike PD, APD incorporates internal gain, which implies on higher electric fields that increase the collected charge. The internal gain improves the signal to electronic noise ratio and provides better energy resolution at lower radiation energy. SiPM consists of an array of small dimension (tens of microns) APD operated in Geiger-Muller (GM) mode. The gain increases with increasing the applied voltage. Over a determined applied voltage the diode enters the GM avalanche mode, in which charges produced in the initial photon interaction are, in principle, multiplied without limit. Thus, a large output pulse can be produced from a single incident photon. Ideally, the size of individual APD cells is small enough, therefore, the probability for a given cell to be hit by a scintillating photon is low and at most a single photon strikes on a single cell. The number of cells producing avalanche is then proportional to the number of scintillation photons. Once common scintillation detectors produce thousands of light photons, the number of cells must be a large multiple of the collected photons to achieve this condition. Therefore, arrays of order of 10^4 cells or more are common. Each individual APD, operating in GM avalanche mode, is connected to a quenching resistor. A gain of order of 10^6 is achieved. The output signal of each cell has approximately the same amplitude, which is set by the uniformity of the cells and the individual quenching resistors. Individual outputs are connected in parallel in order to produce an analog pulse whose amplitude is proportional to the number of detected photons.

II. A.1.1. EXPERIMENT

Figure 1 shows the setup used for the A.1.1. experiment: SiPM characterization. The SP5601 LED driver is connected to the SP5650C SiPM, through an optical fiber and to the SP5600 power supply and amplification unit, which is connected to the DT5720A digitizer.

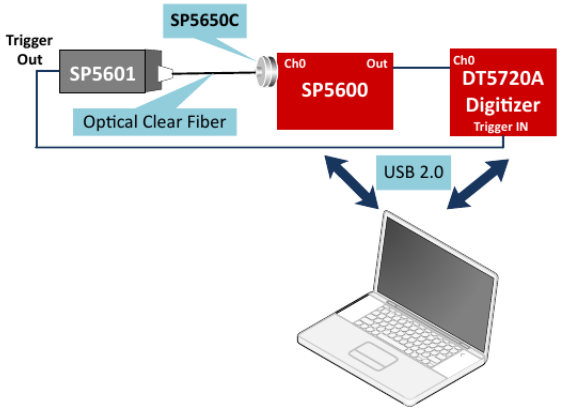

FIG. 1. Scheme of the setup used for the A.1.1 experiment [3].

Table I shows the parameters used for this experiment.

Gain(dB)	32
Bias voltage(V)	55
Pre-gate(ns)	72
Gate(ns)	200
Threshold(mV)	-800

TABLE I. Detector parameters for the A.1.1 experiment. Other parameters were set as default.

With this setup and its respective parameters, we carried out the following experiments.

II.1. Amplitude of the LED driver: light yields simulation

The first experiment was carried out exploring the effect of the amplitude (intensity of incoming light) of the LED driver on the number of peaks detected (cells fired). Figure 2 reports on the detected peaks as a function of the LED driver amplitude. Increasing the amplitude, without varying detector parameters, led to 2 main results:

- Appearance of more peaks (the number of fired cells increases);
- Displacement of the histogram to the right, as a result of increasing the charge collection (figure 3).

Both results are illustrated on figure 3, which includes several spectra as a function of the amplitude of the LED driver. First, as the amplitude increases, a shift to the right (ADC channels) is observed. Second, higher the light intensity is, higher the number of fired cells and consequently the collected charge and, therefore, an increase in the number of peaks is observed.

In figure 2, for the first amplitude values (1, 2) there is no change, but from amplitude 3 to amplitude 7, we can observe an exponential increase.

In figure 3, we can observe 7 peaks for amplitude 5, 14 peaks for amplitude 6 and 25 peaks for amplitude 7. For amplitude 8 and above (up to 10, the maximum amplitude value we can select), the single peaks (fired cells) are no longer distinguishable and the result is a continuum gaussian response. Numbers from 1 to 10 are determined by the number of turns allowed by the selector placed in the front panel of the LED driver. As an example, figure 4 reports on the result obtained with amplitude 6.

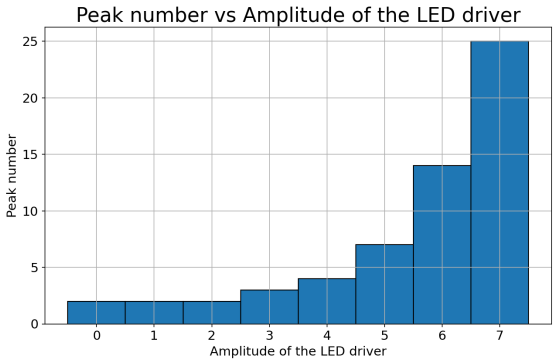

FIG. 2. Number of peaks as a function of the amplitude of the LED driver. From amplitude 8, individual peaks are no longer distinguishable and the result is a continuum response, similar to a single gaussian peak (figure 3).

II.2. Standard deviation versus peak number

Another exploration was to check the dependence between the number of peaks and their respective standard

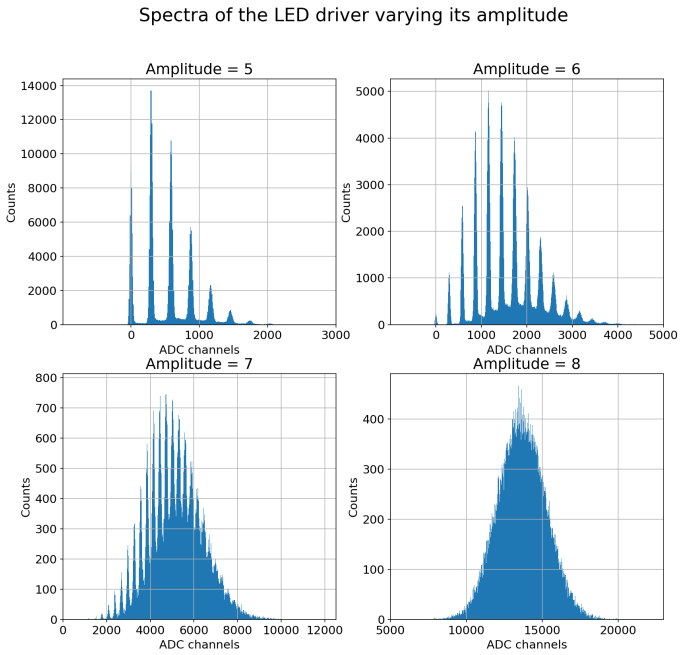

FIG. 3. Several spectra of the LED Driver changing its amplitude (see text for details).

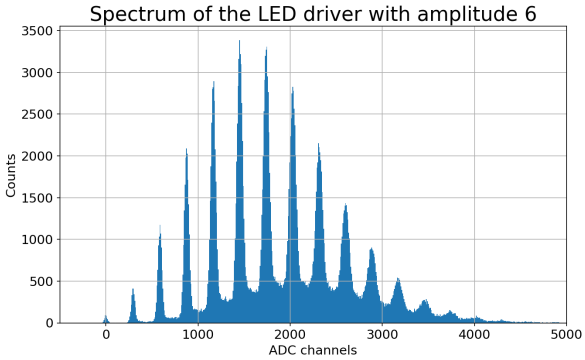

FIG. 4. Histogram obtained with the the LED driver amplitude 6.

deviation. With this proposal, we used the same histogram shown on figure 4. To compute the standard deviation of each peak, such peak was fitted by a gaussian function (using python), and the standard deviation was extracted from the fitting parameters. An example of a gaussian fit is shown on figure 5. The peak number is assigned according to the order of appearance, i.e., in figure 4, the first peak on the left (at channel 0) is defined as peak number 1.

The standard deviation and the variance obtained are shown on figure 6 (a) and (b) as a function of the peak number. From the present data analysis, the standard deviation increases linearly with the peak number, so that the variance increases to the square, which is also appreciable respectively in such plots of figure 6 (a) and (b). Figure 6 (d) is the same of (b) re-scaled and fitted

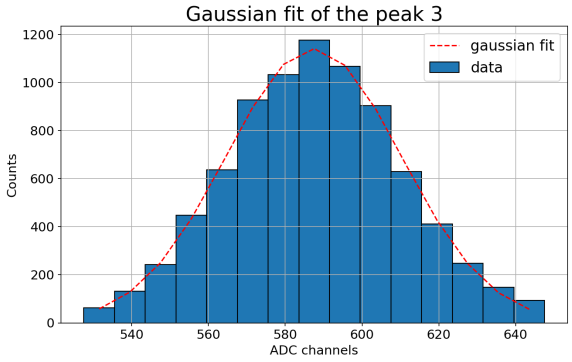

FIG. 5. Gaussian fit to the peak 3 of figure 4 histogram.

with a linear function, in order to compare with CAEN's result (c). In this way, we verify similarities, although we obtain the variance proportional to the square of the peak number N^2 instead of to the peak number N. It is verified by comparing the correlation coefficients obtained in figure 6 (b) (for square fit, $r = 0.992$) and (d) (for linear fit, $r = 0.970$). It is worth to mention that we concentrate our analysis for a lower number of peaks and a convenient scale, where data better agree with a quadratic trend. The results of CAEN A.1.1 experiment follow the scientific paper produced by the research group at Como University (Italy), also reported in Advanced Statistic (D.1) [3]. As it was reported in that paper, the peak width increases with the number N of fired cells with a growth expected to follow a $\sqrt{N}$ law. Notwithstanding, results were obtained considering a different maximum number of resolved peaks.

II.3. Dark counting rate

To measure the dark counting rate, the setup showed on figure 1 was modified:

- LED driver was removed (to avoid spurious events)
- Trigger from SP5600 to DT5720A

The measurements could be taken either by 1) measuring the spectra changing the threshold or 2) using the specific functionality of the software, PSAU staircase. Both options were carried out. For the first option, the histograms were saved and by integrating the counts in all channels (sum) the total number of counts were obtained. This number is also reported by the software, which is in agreement with the one computed from the histograms.

Figure 7 (a) shows the results for threshold values from 0 to -60mV. Figure 7 (b) and (c) show the results obtained with the second method and the reference result from CAEN's catalog [3]. We can see that using both methods, a decreasing pattern is obtained, although the structures of such decreasing are different. Different measurements were carried out varying the gate without obtaining the reference staircase structure.

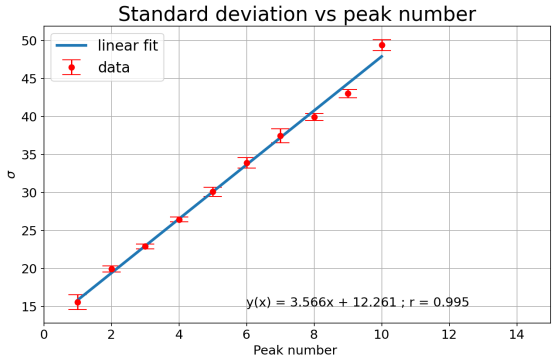

(a)Standard deviation as a function of the peak number

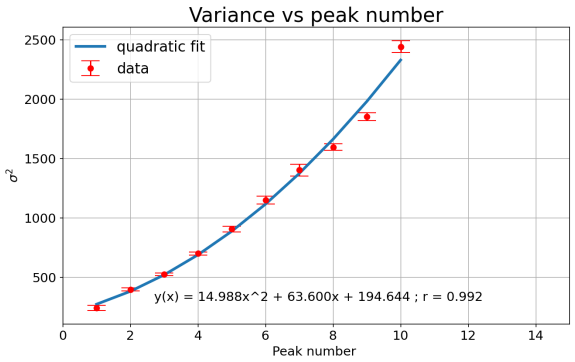

(b)Variance as a function of the peak number

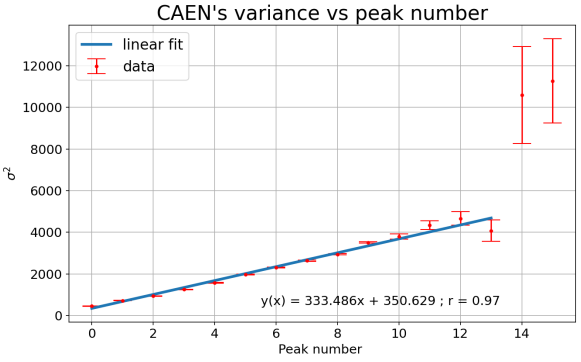

(c)Result extracted from CAEN's catalog [3].

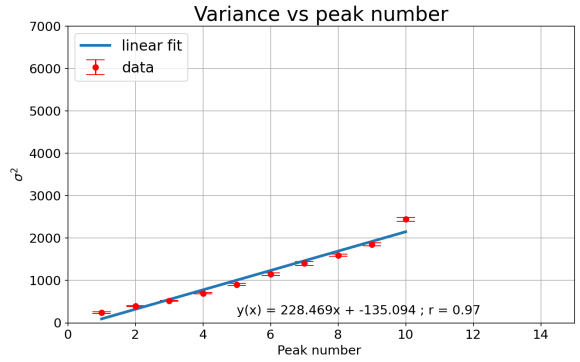

(d)Variance as a function of the peak number (for lower peak numbers and using a similar scale to CAEN's plot (c)).

FIG. 6. Standard deviation and variance as a function of the peaks number. Fit equations and the correlation coefficients are also reported.

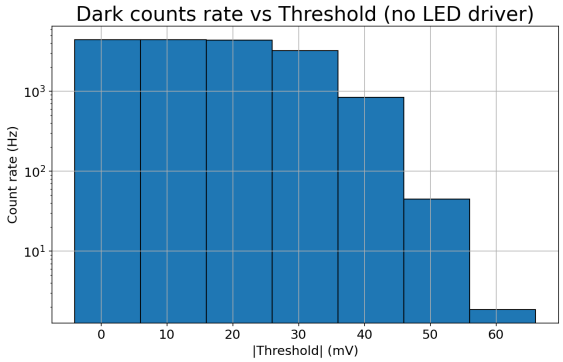

(a)Result using method (1)

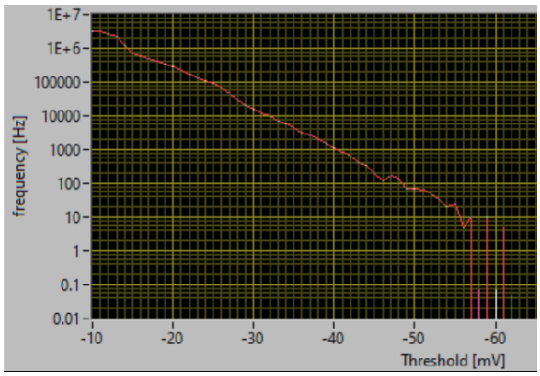

(b)Result using method (2)

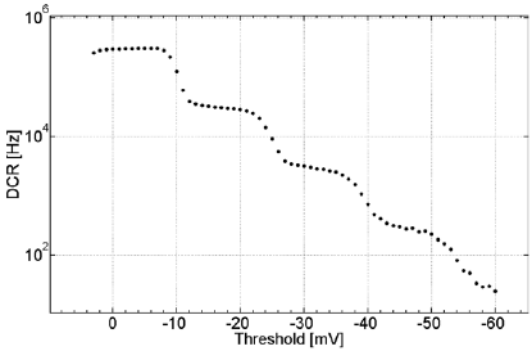

(c)CAEN's result.

FIG. 7. DCR results obtained without (a) and with (b) using the software, compared to reference results from CAEN (c). The measuring time was 30s and the LED driver was unplugged.

III. B.1.5 EXPERIMENT

Figure 8 shows a scheme of the setup used for the B.1.5 experiment. Now, instead of using the LED driver, we have a ^{137}Cs gamma source coupled individually to BGO, LYSO(Ce) and CsI(Tl) crystals, which are responsible for the light yield. The image was extracted from the CAEN's educational catalog [3]. Notwithstanding, connections have been modified, as it is indicated in figure 8. The goal was to keep the original amplitude of the signal coming from the detector, allowing us to inspect such signal on the scope, before and after being processed by SP5600 amplification unit.

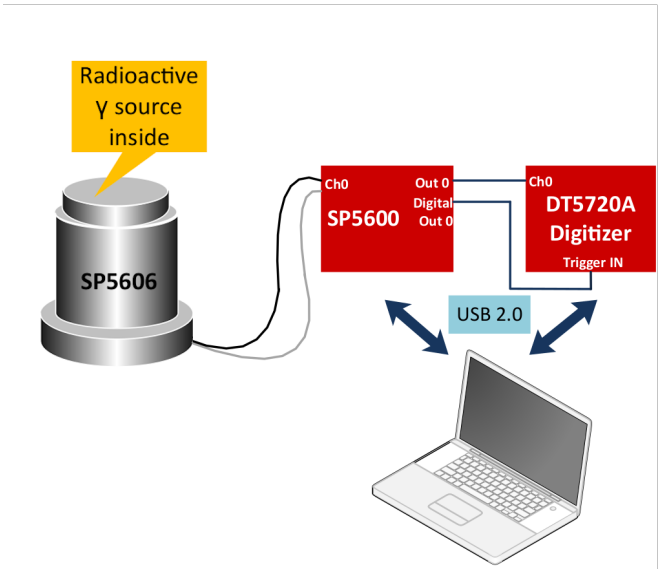

FIG. 8. Scheme of the setup used for the B.1.5 experiment. Here, we modified connections in order to keep the amplitude of the original signal, coming from detector (we did not divide it).

With the setup of figure 8, measurements using ^{137}Cs were carried out, varying the scintillating crystal and keeping the same detector configuration. The main parameters used for this experiment are reported in table II. The gain is set to minimize the noise, and the threshold was set to optimize data acquisition (counting rate). The detector support SP5606 was conveniently adapted to increase the distance between source and detector and reduce piling events up.

Gain(dB)	1
Threshold(mV)	-17
Bias voltage(V)	55.57

TABLE II. Detector parameters for the B.1.5 experiment. Gate and pre-gate depend on the crystal to optimize the signal measurement. Other parameters were set to the default ones.

Our spectra are shown on figure 9, and are compared with the CAEN catalog ones. Spectra are very similar, both display similar features. Note that in our case, due to the applied threshold, there is no counts near channel 0. To further characterize the scintillators, the resolutions $R \equiv FWHM/<\text{channel}>$, have been estimated and reported on next section.

III.1. Resolution

To compute R, the ^{137}Cs photopeak was fitted to a gaussian function, for each spectrum of figure 9. The resolutions are shown on figure 10 and in table III, where they are compared to the reference values of light yield. From figure 11, we can estimate and verify the values

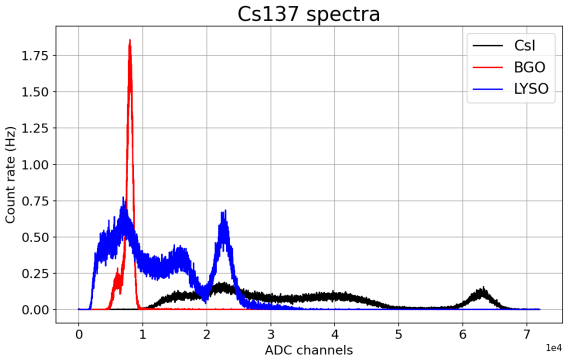

(a)Our results.

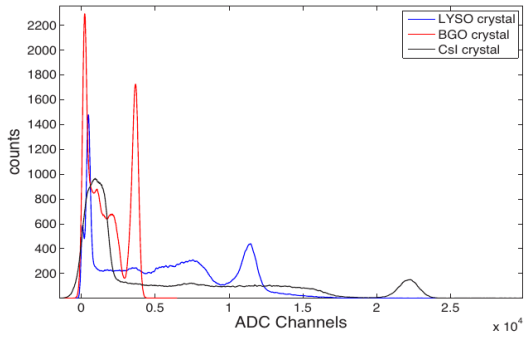

(b)CAEN's resuts.

FIG. 9. ^{137}Cs gamma spectra obtained in our laboratory (a) compared to CAEN's result (b). The measurements were carried out during 600s for the CsI and during 200s for the BGO and the LYSO crystals.

obtained. According to the tabulated light yield, considering just statistical fluctuations, the lowest (best) resolution should correspond to CsI, then LYSO and finally BGO. Our data show this sequence, however, the BGO and LYSO resolutions are quite similar (even compatible) and worst than CsI, which presents a quite good resolution.

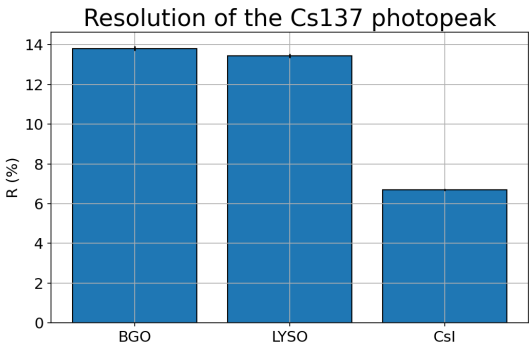

FIG. 10. Resolution of the ^{137}Cs gamma photopeak, obtained for the different scintillators.

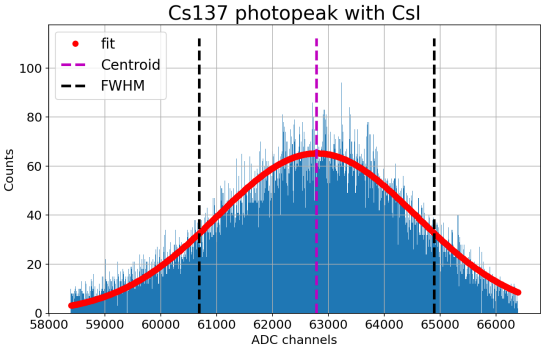

(a)CsI (best resolution).

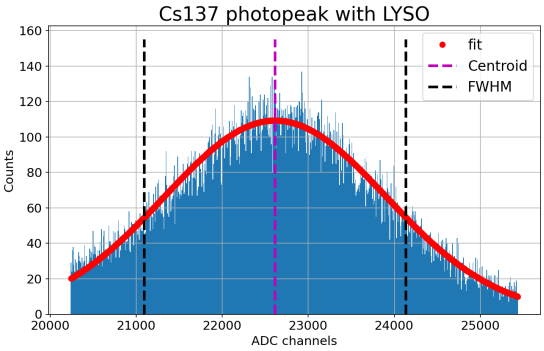

(b)LYSO.

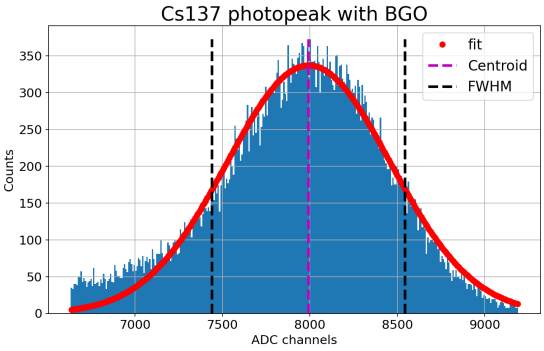

(c)BGO (worst resolution).

FIG. 11. ^{137}Cs gamma photopeak, obtained for different crystals. Solid lines represent gaussian fits; vertical dashed lines are eye guides to estimate the centroid and the FWHM.

	BGO	LYSO	CsI
$FWHM$	1104(10)	3039(30)	420(3)10[1]
$<$ channels $>$	7992(4)	22614(9)	62790(12)
$R(\%)$	13.81(11)	13.43(10)	6.69(5)
Light yield (ref)	8200	27000	52000

TABLE III. Resolution of the ^{137}Cs gamma photopeak for the different scintillators. Tabulated light yields are used as reference.

III.2. Pulse High and Pulse Shape Analysis for Light Yield Estimation

Looking for establishing a relation between the light yield and the signal (charge/voltage) integration, we proceed with pulse high analysis (PHA) and pulse shape analysis (PSA). The decay time of signals was measured using the oscilloscope, in two different ways (for each crystal):

- signal coming directly from the detector
- signal coming from the SP5600

The gain was set to its minimum value in order to decrease the noise level of signals. The signal from the detector was divided into 2 signals, one goes to the SP5600 and the other one goes directly to the first channel of the oscilloscope (see Fig. 12). The output signal from the SP5600, goes to the second channel of the oscilloscope.

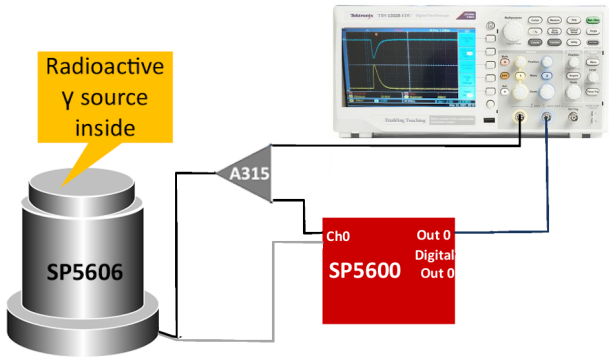

FIG. 12. Scheme of the alternative setup used for the B.1.5 experiment. Here, we modified connections in order to measure the signal coming from the detector and from the SP5600 module at the same time.

Figure 13 shows some examples of signals obtained from the three cases (crystals). The threshold of the SP5600 was modified (for each crystal) as well as the oscilloscope trigger (set on signals coming from SP5600). The goal was to capture a signal related to the photopeak (for each case). Thus, the signal from the SP5600 is chosen for the trigger, which selects a signal with the maximum possible amplitude and with a relatively high frequency of appearance. This process was carried out with caution to avoid choosing spurious events such as pile up, sum peak, among others. Figure 14 compares (in the same plot) the pulse shape of the signals (a) directly from the detector and (b) from SP5600, for the different crystals.

The rise and decay times of the signals are compared in figure 15. In table IV, in addition to signals decay times,

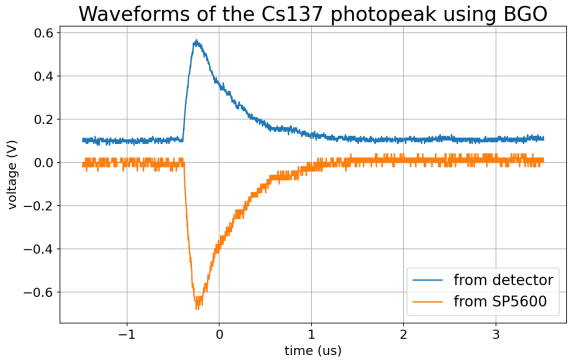

(a)BGO.

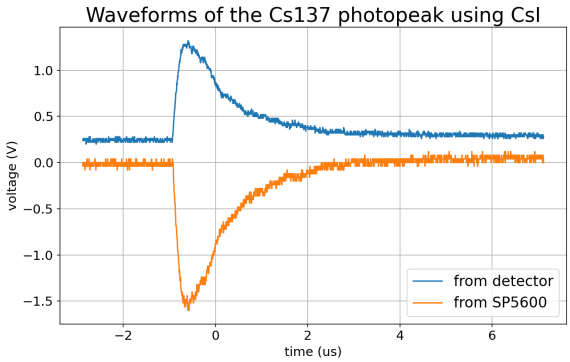

(b)CsI.

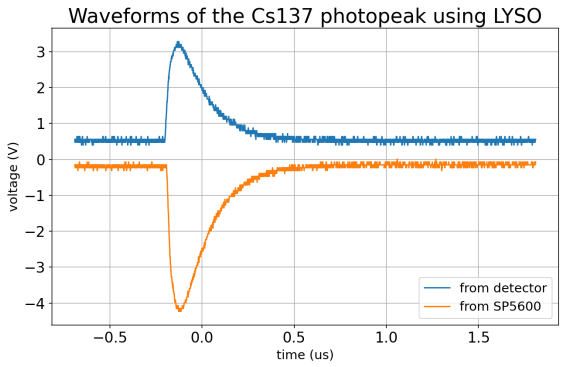

(c)LYSO.

FIG. 13. Signals produced by ^{137}Cs gamma interaction on different crystals. Signals are measured directly from the detector (blue) and after being processed by the SP5600 (yellow), for each crystal. Both signals are measured at the same time.

we present the maximum amplitude (maximum voltage - pulse high) and the peak integral. Integrals are performed using python. Decay times of pulses before and after being processed by SP5600 are quite similar. Fluctuations are mostly due to the determination of base line restoring. In this sense, a fine tuning can be processed by software analyses. Regarding to the amplitude, after being processed by SP5600, it is increased by an average factor around 1.5, for all cases. The crystal with higher

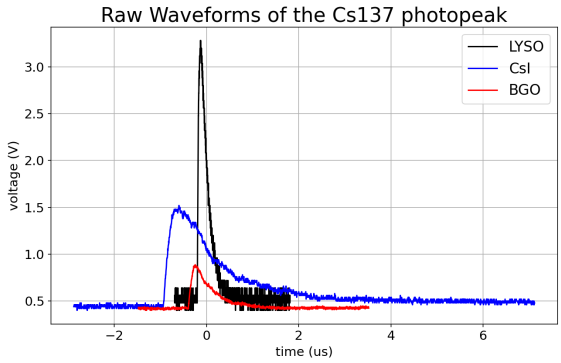

(a)Signals directly from the detector (for different crystals).

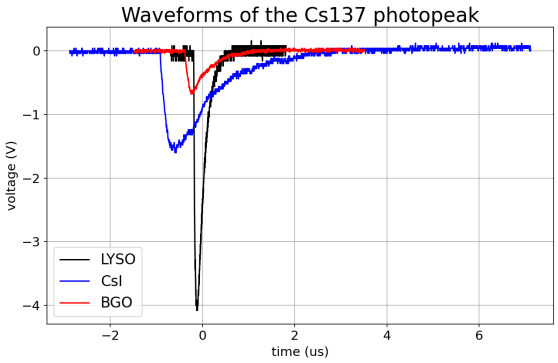

(b)Signals from SP5600 (for different crystals).

FIG. 14. Signals of ^{137}Cs gamma interaction (photopeak) with the different crystals. Signals were measured with the oscilloscope before (left) and after (right) being processed by the SP5600.

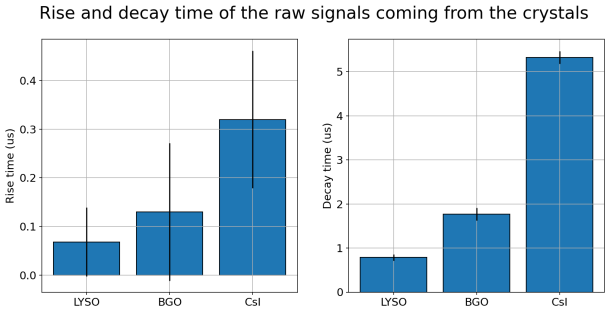

(a)Signals from the detector.

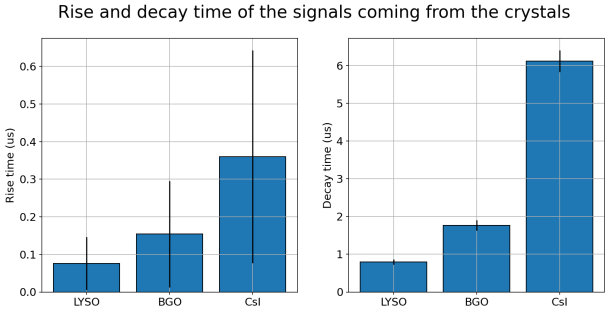

(b)Signals from the SP5600.

FIG. 15. Rise and decay time for signals obtained directly from the detector (a) and after being process by the SP5600 (b). The splitter was used for the signals that comes out of the SP5600 to divide the signal into two: one sent to the oscilloscope, and the other to the DT5720A.

Decay time (μs)	LYSO	BGO	CsI
Signal from SP5600	0.79(4)	1.78(14)	6.12(28)
Signal from detector	0.79(7)	1.77(14)	5.32(14)
decay time ratio	1.00(7)	1.01(11)	1.15(6)
Amplitude SP5600 (V)	4.08(28)	0.68(6)	1.60(14)
Amplitude detector(V)	2.71(14)	0.4640(28)	1.020(6)
Amplitude ratio	1.51(13)	1.466(28)	1.57(14)
Peak integral (V·μs)	0.98(7)	0.34(7)	1.9(6)

TABLE IV. Measured decay times and amplitudes of signals, before and after the SP5600. Here the ratios refer to (preamp output)/(preamp input) values obtained for the same crystal. The peak integrals (of SP5600 output signals) are also reported.

Decay time ratio	BGO/CsI	LYSO/CsI	LYSO/BGO
Signal from SP5600	0.291(26)	0.129(9)	0.44(4)
Signal from detector	0.333(28)	0.148(14)	0.45(5)
Amplitude ratio SP5600	0.43(5)	2.55(28)	6.0(7)
Amplitude ratio detector	0.455(4)	2.66(14)	5.8(3)

TABLE V. Measured decay time and amplitude (pulse high). Here, the ratios are calculated between each couple of different scintillators, in two cases: i) ratios between input signals (before SP5600) and ii) ratios between output signals (after SP5600).

decay time is CsI, then BGO, which presents the lower amplitude (pulse high), and finally LYSO, which presents the higher amplitude (pulse high). For comparisons, the ratio of the decay times and amplitudes, between different scintillators, have also been calculated. These ratios are calculated for two cases: i) ratios between values of the input signals (before SP5600) and ii) ratios between values of the output signals (after SP5600). The results are shown in table V.

In table VI, values of the (voltage) integral ratios are compared to the reference light yield ratio. In the same table, the peak position ratio obtained from the histograms (figure 9) are compared to the reference values [3]. The lowest integral ratio was obtained for BGO/CsI, while the highest is obtained for LYSO/BGO. The sequence (from smallest to highest) of signals integral ratio is the same obtained in [3] for light yield and peak position ratios. Variations between results reported here and the reference ones should be mostly related to statistical fluctuations of the inspected signals with respect to the average ^{137}Cs gamma photopeak (centroid) for each case.

Parameter	BGO/ CsI	LYSO/CsI	LYSO/BGO
Peak integral ratio	0.18(7)	0.52(17)	2.9(6)
Light yield ratio (ref)	0.16	0.52	3.29
Peak pos. ratio (ours)	0.12728(7)	0.3602(16)	2.8295(18)
Peak pos. ratio (ref)	∼0.16	∼0.51	∼3.11

TABLE VI. Peak integral, reference light yield and peak position ratios. The peak integral ratios are calculated considering just the output signals.

IV. CONCLUSIONS

We report on a combined analysis for the experiments of SiPM characterization (A.1.1) and comparison of different scintillating crystals: light yield, decay time and resolution (B.1.5).

In the experiment A.1.1, using the SP5601 LED driver, we represent (Figs. 2 and 3) the increase of the number of peaks as a function of its (LED driver) amplitude, up to the limit of resolution (limit of distinguishing between peaks - Figure 3). Increasing amplitude implies on more peaks, which move forward (to the right) in the spectra (ADC channels), which is related to the amount of collected charge. Higher the LED driver amplitude (intensity) is, more events are generated, more cells are fired (at the same time window), and, therefore, more charge is being integrated. Figures 5 and 6 report on the sigma and variance of each peak as a function of the peak number. For a low number of peaks, we observe linearity in terms of sigma and quadratic behaviour in terms of variance. The SiPM measures the light intensity from the number of fired cells up to a limit determined by increasing dark counts, after pulses and optical cross talk.

Regarding the experiment B.1.5, when using ^{137}Cs gamma source coupled individually to BGO, LYSO(Ce) and CsI(Tl) crystals with a constant volume (6x6x15mm^3), the light yield is due to a ^{137}Cs gamma interaction with the respective crystals. Once more a spectroscopic response is analyzed. First, we reproduce spectral response for the three available crystals (figure 9). Afterwards, we concentrate on resolution. According to the light yield and considering just statistical fluctuations, the lowest (best) resolution should correspond to CsI, which agrees with our data. Furthermore, the CsI crystal presents a very good resolution. The resolution value obtained for LYSO is quite close (compatible) to the BGO ones (see table III) and they are both worst than the CsI resolution. It could be due to some extra systematical error/noise sources, different from the statistical ones. It is worth to mention that we have not removed the background of the spectra, once we assumed the effect should be the same for all cases.

We continue our experiments looking for estimating the light yield (during a determined (photopeak) event). To investigate on that, we study charge/voltage signals. Thus, we perform pulse high analysis (PHA) and pulse shape analysis (PSA) of signals coming directly from the detector (charge) and after passing through the SP5600 (voltage). Figures 13 and 14 show the results obtained from the scope. We can verify that variations on the decay time are mostly connected to the determination of base line restoring. Regarding to the amplitude, after being processed by SP5600, it is increased by an average factor around 1.5, for all cases (crystals). The crystal with the higher decay time is CsI, then BGO, which presents the lower amplitude, and LYSO, which presents the higher amplitude. For comparisons, the ratio of the decay times, for different scintillators, have also been calculated and the results are shown in table V. The decay time results is conceptually different from reference values [3] that account for how long it takes the excited states to de-excite and give off light. They should be correlated and such a correlation would be a topic of value for future studies.

In table V, we also present the amplitude (pulse high) ratios. The lower amplitude (pulse high) ratios were obtained for BGO/CsI, while the higher is obtained for LYSO/BGO. The sequence of such ratios is the same obtained in [3] for light yield and peak position ratio (table VI). Variations between results reported here and the reference ones should be mostly related to statistical fluctuations of the inspected signals with respect to the average ^{137}Cs gamma photopeak (centroid) for each case.

V. REFERENCES

[1] Glenn F. Knoll *Radiation Detection and Measurements*. 4ª edition. John Wiley & Sons, Inc., 2010. ISBN: 978-0-470-13148-0.

[2] S.M. Sze. *Physics of Semiconductor Devices*. 2ª edition. New Jersey: Willey-interscience publication, 1981.

[3] CAEN. *CAEN Educational catalog*. 2016 edition.

VI. ERROR CONVENTION

The error notation used here is bracket notation: $11.5 \pm 1.2 \equiv 11.5(12)$. Regarding to the calculated magnitudes, relative quadratic error propagation have been applied. The error is shown with only 2 significant digits, if the first digit is lower than 3 (1,2) and with only 1 significant digit for the rest of the cases.